Climatic trends in fog occurrence over the Indo-Gangetic plains

Article *in* International Journal of Climatology · October 2019

DOI: 10.1002/joc.6317

CITATIONS
29

READS
486

3 authors:

Saumya Kutty
Jawaharlal Nehru University
4 PUBLICATIONS **74** CITATIONS
SEE PROFILE

A P Dimri
Jawaharlal Nehru University
301 PUBLICATIONS **7,789** CITATIONS
SEE PROFILE

Ismail Gultepe
University of Ontario Institute of Technology
189 PUBLICATIONS **5,614** CITATIONS
SEE PROFILE

Received: 28 February 2019 | Revised: 17 September 2019 | Accepted: 17 September 2019

DOI: 10.1002/joc.6317

RESEARCH ARTICLE

International Journal of Climatology RMetS

Climatic trends in fog occurrence over the Indo-Gangetic plains

Saumya Govindan Kutty[1] | **Ashok Priyadarshan Dimri**[1] | **Ismail Gultepe**[2,3]

[1]School of Environmental Sciences, Jawaharlal Nehru University, New Delhi, India

[2]OBRS, Meteorological Research Division, ECCC, Toronto, Ontario, Canada

[3]Faculty of Engineering and Physical Science, UOIT, Oshawa, Ontario, Canada

Correspondence
Ashok Priyadarshan Dimri, School of Environmental Sciences, Jawaharlal Nehru University, New Delhi-110067, India.
Email: apdimri@hotmail.com

Funding information
University Grants Commission funding for Senior Research Fellowship and Jawaharlal Nehru University

Abstract

The Indo-Gangetic plains (IGP) in India witness widespread fog during winter months of December–January–February (DJF) since 1970s at temperatures between 5 and 20°C. Despite its vast spatial extent, the localized physical nature of fog over various time and space scales limits successful attempts of its accurate prediction. This poses a challenge towards reducing calamities and huge economic losses associated with the consequent visibility degradation. Increasing rate of urbanization and both enhanced natural and anthropogenic forcing influence fog formation, persistence, and dissipation. It is imperative to understand the associated changes in fog trends to ascertain the effect of these forcing on fog and quantify its prediction. Therefore, the trends in fog occurrence over the Indo-Gangetic plains are assessed for a period of 37 years from 1977/1978–2013/2014 (DJF). A statistically significant increasing trend in fog frequency is found to be related to changes in associated meteorological parameters. The shift of visibility around year of 1998 is indicated by important changes occurred in temperature, humidity, and wind speed. Distinct patterns before and after 1998 are observed for fog visibility conditions and that may have significant implications for weather forecasts and local climate change.

KEYWORDS
fog trend, Indo-Gangetic plains, regime shift, visibility

1 | INTRODUCTION

Fog is a common weather phenomenon in the Indo-Gangetic plains (IGP) in India during winter and covers a stretch of ~1,500 km in length and ~400 km in width (Gautam *et al*., 2007). The consequent reduction in visibility (Vis) to below 1 km causes huge economic losses in the transportation and agriculture sectors (Business Standard, 2013; The Economic Times, 2017). The densely populated plains are a source of anthropogenic pollutants including black carbon and sulphates in the winter (Di Girolamo *et al*., 2004). Other sources include biomass burning and dust storms. Low temperatures and high pressure conditions following the passage of synoptic weather systems called Western disturbances (WDs), trap these pollutants within the trough like topography of the region creating conditions conducive for fog and haze during DJF (December, January, and February).

Radiative cooling at night combined with low wind speeds and moisture availability contribute to radiation fog, one of the two most commonly observed fog types in the IGP. The other type, advection fog is observed prior to passage of WDs (Sawaisarje *et al*., 2014). Studies have shown positive trends in fog frequency over the region with an increase in aerosol loading (Jenamani, 2007; Ganguly *et al*., 2012; Kaskaoutis *et al*., 2014). The changing climate scenarios with associated natural and anthropogenic forcing have influenced fog mechanism resulting in more frequent and persistent occurrences. In contrast, a decrease in fog cover has also been observed over cities and attributed to urban heat island effect (Gautam and Singh, 2018). These indicate

the localized nature of fog and the role of land surface processes in fog formation and dissipation.

Ground based observation campaigns have been carried out in IGP (Ghude *et al*., 2017) and elsewhere in the world (Gultepe *et al*., 2008, 2009; Giulianelli *et al*., 2014; Dupont *et al*., 2016; Price *et al*., 2018) in an attempt to quantify the extent of influence of these factors on fog dynamics and in particular on Vis and microphysics during fog episodes. Though they have provided insight into fog processes, its accurate prediction is still a challenge. Gultepe *et al*. (2006, 2007), in addition to multiple interactions of various fog occurring conditions, stated that without accurate prediction of droplet number concentration (N_d), numerical weather predictions (NWPs) cannot predict accurate Vis, and this needs to be researched.

Fog forecasting has evolved with the advent of novel techniques including statistical approaches, machine learning with artificial neural networks (ANN) and numerical weather prediction (NWP) models (Gultepe *et al*., 2018). The challenge for dynamical forecasting lies in the inability of models to adequately represent forcing factors at finer resolutions and for statistical methods, in defining the occurrence and intensity of fog given the latter's categorical nature and threshold dependency. Zhou and Du (2010) explored a diagnostic fog forecasting method based on five model variables and found that the fog forecast efficiency increased with larger ensemble size and multi-model approach from an initial equitable threat score (ETS) of 0.063 to 0.334. However, model effectiveness in predicting fog occurrence within different thresholds was not assessed.

Chaudhuri *et al*. (2015) applied different ANN approaches for nowcasting Vis during fog at various airports of India and also analysed their sensitivity to station altitudes and found that the multilayer perceptron (MLP) model performs well in nowcasting Vis with 6 hr lead time. However, a sensitivity to station altitudes was observed concluding that the MLP model though location specific, may be used in nowcasting Vis during fog. Dutta and Chaudhuri (2015) used the decision tree approach to develop MP model with back propagation learning technique and achieved forecast for dense Vis within a distance of 50 m. The selected parameters included both meteorological factors and air pollutants which stressed on the need for consistent, high-resolution data sets for input in models. multiple linear regression (MLR) approach was used by LaDochy (2005) to assess the relationship between fog frequencies and temperature as well as total suspended particulates (TSP) at two sites in Los Angeles. Further, to assess possible influence of Pacific Decadal Oscillation (PDO); stepwise MLR was also used with the above factors along with sea surface temperature as independent variables (LaDochy, 2005; Witiw and LaDochy, 2008). These studies suggested that variances at two sites were explained by TSP and PDO indexes at 36 and 33% and the analysis was limited to fog occurrences with Vis <400 m. The analysis utilized a long data set spanning from 1950s to 2004 and inclusion of these long-term trends in estimating regression equations provided better outcomes. However, analysis of such long-term trends is limited within the Indian context. Madan *et al*. (2000) applied different approaches including auto regression, multiple regression, climatology, and persistence with Vis as dependent variable. The study was limited to a 7-year period from 1984 to 1990. Their results showed that Vis forecasts had large deviations and results were not found to be satisfactory for climatic changes. Mohapatra and Thulasi Das (1998) also explored objective techniques including persistence, synoptic, statistical, and composite method using 10-year data set over Bangalore, India. The composite method, where threshold values as well as threshold values of change in fog predictors were considered, was found to perform comparatively better than other methods. Bhowmik *et al*. (2004) used the composite method with multiple discriminant analysis over Delhi from 1997 to 2000 and stress out that a majority of fog occurrences were associated with backing condition of wind between 1,000 and 700 hPa. In-spite of good skill scores, the forecast was slightly under-predicted in the development data set and over-predicted in case of independent data set. The inaccurate performance of results stressed that importance of analysing long-term trends in fog occurrence for adequate representation of natural and anthropogenic forcing in prediction models is needed.

Most studies are limited to point locations, in particular airports due to data limitations elsewhere. Therefore, results derived from these studies are limited in their spatial extent. Fog prediction over IGP was also attempted using a NWP model (NCMRWF Unified Model, NCUM) with fixed aerosol content (Singh *et al*., 2018). The model was based on limited observations taken during December 2014–January 2015 and the predicted Vis values were higher than observations. More recently, a study by Arun *et al*. (2018) used multi-satellite data based fog detection scheme and fog stability index (FSI) for effective fog prediction over IGP. Fog as well as non-fog conditions were observed and results were agreed with observations to a great extent. However, data discontinuity of polar satellite overpasses limits the efficiency of satellite based studies. Srivastava *et al*. (2016) analysed the spatio-temporal variability of fog over IGP and found an increase in fog frequency. However, this study did not attempt to look into crucial aspects of fog occurrence, including presence of possible regimes and differentiate between fog and non-fog days. The present study would pave way for the assessment of long-term fog occurrence and Vis evaluation patterns using observations from 10 weather stations along southern part of Himalayan

plateau, and quantify changes in meteorological factors affecting fog occurrence. Observations of fog-related parameters were obtained from December 1977 to February 2014. The specific objectives of the study are as follows:

- To observe the trends in fog occurrence and associated meteorological parameters in the IGP of India.
- To evaluate Vis versus dew point depression, $T_{dep} = T_{db} - T_d$; (where T_{db} is dry bulb temperature and T_d is dew point temperature), applicable to a new climatic analysis classification.
- To assess presence of possible regimes within the study period since 1970s and emphasize its impact on weather forecast and local climate change.

The Introduction section provides overall summary of the earlier work of the current problem. Then, Data and Methods section explain the data and observations as well as the analysis used. Section 3 as Results and Discussions provide required analysis results and discussed issues that may arise in the analysis. Finally, Conclusions (Section 4) itemize possible lessons learned from the results of this work.

2 | DATA AND METHODS

2.1 | Data

For estimation of fog occurrence and frequency, station-based meteorological data set obtained from the National Centers for Environmental Information (NCEI), a repository of land, ocean and atmospheric data maintained by National Oceanic and Atmospheric Administration (NOAA) has been utilized. Daily as well as three hourly data of meteorological variables namely T_{db}, T_d, wind speed (U), Vis, maximum and minimum temperatures (T_{amax} and T_{amin}), and relative humidity (RH) were obtained for 10 meteorological stations over IGP (Figure 1 [Stations 1–10]). These stations were chosen as per data availability and span over Punjab, Haryana, Delhi, Uttar Pradesh, and Bihar. As low Vis may be attributed to factors other than fog, including haze, rain, and snow (Gultepe *et al*., 2018), fog occurrence is assumed when three conditions are satisfied: (a) the Vis <1,000 m, (b) the present weather codes indicate fog, and (3) no precipitation exist. For the daily data set, fog occurrence/non-occurrence is derived from indicators (1 = yes and 0 = no/not reported). As these data sets are derived from the synoptic/hourly observations contained in United States Air Force Surface data and Federal Climate Complex Integrated Surface Data (ISD), they undergo extensive automated quality control to correctly "decode" as much of the synoptic data as possible, and to eliminate many of the random errors found in the original data. Then, these data are quality controlled further as the summary of day data is derived. In deriving the summary of day data, a minimum of four observations for the day must be present (allows for stations which report four synoptic observations per day). Information on quality control and further description of data may be found at (https://www.ncdc.noaa.gov/isd/data-access). Historical data are generally available for 1929 to the present, with data from 1973 to the present being the most complete. Keeping this in mind, fog occurrence during boreal winter (DJF) from 1977/1978 to 2013/2014 is considered in this study.

2.2 | Method

Fog frequency (F_f) is calculated by dividing the number of fog days by the number of days in DJF for each year. The time series and averages for all stations are analysed for possible regime shifts by applying a regime shift indicator (RSI) test proposed by Rodionov (2004). This test uses a *sequential t-test analysis* and determines the timing of regime shifts by means of calculating the *regime shift index* (RSI) (Rodionov, 2004; Syed *et al*., 2012). The method ensures minimum delay in estimating probability of a regime shift and monitoring the change in probability over time. This

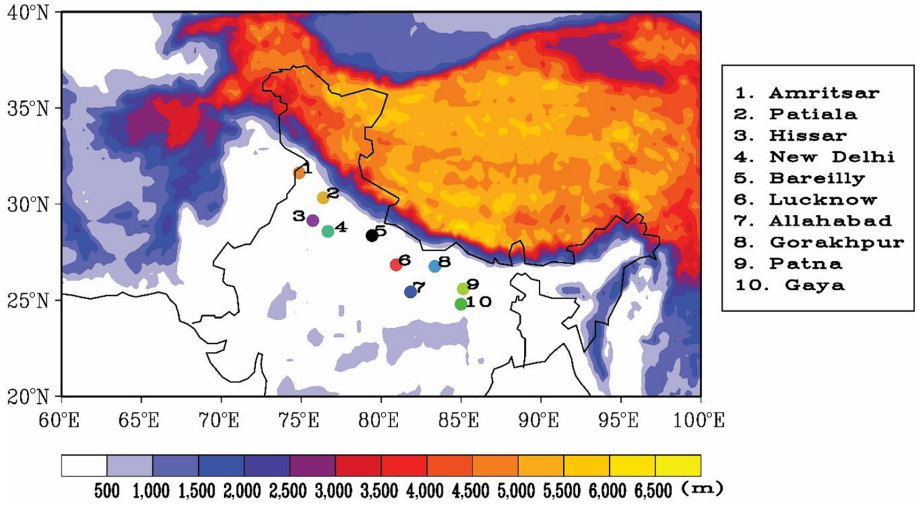

FIGURE 1 Topography over the study area and location of the stations in the Indo-Gangetic plains. The study period is from 1977/1978 to 2013/2014 (DJF). The stations have been chosen as per data availability and obtained from the National Centers for Environmental Information (NCEI), a data repository maintained by NOAA [Colour figure can be viewed at wileyonlinelibrary.com]

method successfully deals with the problem of deterioration of the test statistics towards the ends of time series and can handle data in the form of absolute values as well as anomalies. For each new observation, a test is performed to determine the validity of the null hypothesis, H_0 (the existence of a regime shift). There are three possible outcomes of the test: accept H_0, reject H_0, or keep testing. It involves determining the difference (D) between mean values of two subsequent regimes that would be statistically significant according to the Student's t test:

$$D = t\sqrt{\left(2\sigma_L{}^2/L\right)} \quad (1)$$

where t is the value of t-distribution with 2L-2 degrees of freedom at the given probability level (p) and the cut off length (L) as 10 for the present study. The cut off length determines the minimum length of regimes for which magnitude of shifts remains intact. With an increase in magnitude of shift, regimes shorter than L years also can pass the test. Therefore, L has to be chosen carefully. Here, L is chosen as 10 based on frequency analysis of the Vis time series during fog averaged over IGP for the period 1977/1978–2013/2014. The ensemble empirical mode decomposition (EEMD) method (Wu and Huang, 2009) used for this purpose decomposes the data locally into different oscillatory components called intrinsic mode functions (IMFs) which are all in the time domain and of same length as original signal. This allows preservation of varying frequency in time. EEMD further takes care of mode mixing by performing the empirical mode decomposition (EMD) over an ensemble of the signal plus Gaussian white noise. The lower IMFs represent fast oscillation components while the higher IMFs represent slow oscillations. By means of a sifting process, mean of signal and each consecutive IMF is removed until no cyclic component is left. IMF is essentially a function that has only one extreme between zero crossings and a mean value of zero. Fourier analysis, which helps identify definite frequency peaks in the time series is applied to the significant IMFs which further provides the basis for selection of the cut off length.

The calculation for difference (D) is followed by calculating the mean μ_{R1} of the initial L values of the time series as an estimate for regime R_1 and the levels that should be reached in the subsequent L years to qualify for a shift to regime R_2, $\mu'_{R2} = \mu_{R1} \pm D$. Then,

$$\mu'_{R2} = \mu_{R1} + D \text{ for } i = L+1 \quad (2)$$

or

$$\mu'_{R2} = \mu_{R1} - D \text{ for } i = L+1 \quad (3)$$

where a regime shift is indicated at say, year j when the value, $i = L + 1$ is greater than $\mu'_{R2} = \mu_{R1} + D$ or less than $\mu'_{R2} = \mu_{R1} - D$.

In order to further confirm or reject the null hypothesis of existence of a regime shift at $i = j$, each new value x_i is used to compute the RSI which reflects the change in confidence of a regime shift at year j.

$$\mathrm{RSI}_{i,j} = \sum_{i=j}^{j+m} \frac{x^{i*}}{L\sigma^L}, m = 0, 1, \ldots, L-1$$

where $x_i{}^* = x_i - \mu'_{R2}$ if the shift is up or $x_i{}^* = \mu'_{R2} - x_i$ if the shift is down.

The confidence that a shift occurred depends on whether the anomaly is of the same sign as the one at the time of regime shift. If true, the confidence increases while if sign reverses, the test for regime shift at year j has failed and the test is to be continued for $i > j$.

Fog frequency and associated meteorological parameters are assessed for the 10 regimes. Student's paired t test is applied for test significance at 5% level where the null hypothesis of zero difference is considered between the

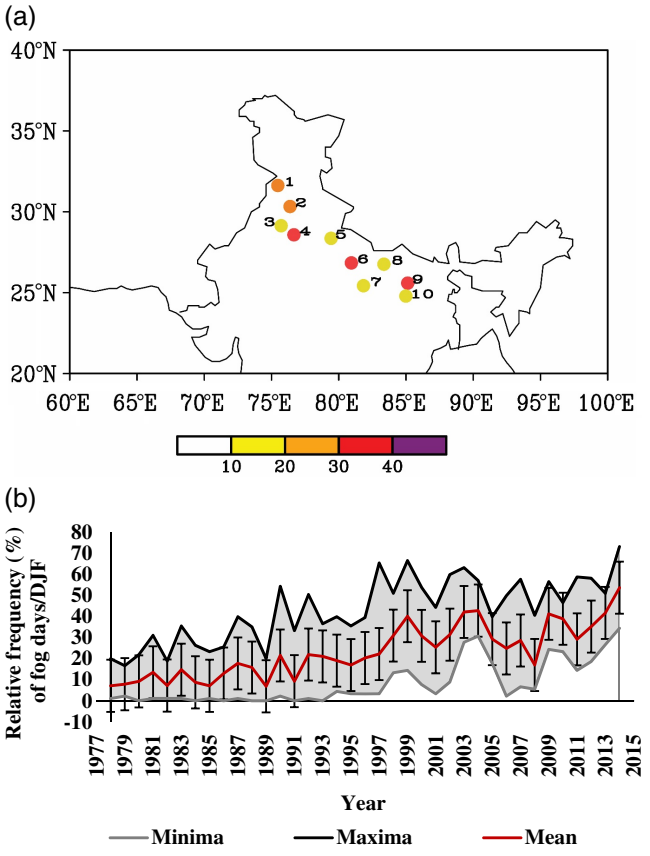

FIGURE 2 Frequency (%) of fog days with respect to DJF during 1977/1978 to 2013/2014 over 10 stations in the IGP with <50% missing values of all days in DJF. (a) Spatial distribution and (b) Time series with mean (red), maxima (black) and minima (Grey) corresponding to the 10 stations; bars correspond to ±1 standard deviation. Each year corresponds to DJF, that is, January–February of that year and December of previous year. The fog frequency varies between 10–40% (a) and temporally, has an increasing trend (b). A regime shift is observed at year 1998 [Colour figure can be viewed at wileyonlinelibrary.com]

distinct regimes obtained thus. Trends are assessed using *Mann–Kendall–Theil–Sen slope estimator* (Kendall, 1938; Sen, 1968). Then, the relations between Vis and meteorological parameters for fog and non-fog days are derived for all the regimes.

3 | RESULTS AND DISCUSSION

Results are obtained over 37 years from 1977/1978 to 2013/2014. First, we plot relative frequency of fog days with respect to DJF versus years. Then, spatio-temporal pattern of fog occurrence in the IGP is shown in Figure 2. The frequency varies between 10 and 40% and major cities including New Delhi (4), Lucknow (6), and Patna (9) correspond to maximum frequency range of 30–40% with 37.4, 30.5, and 35.8%, respectively (Figure 2a). This is followed by Amritsar (1) and Patiala (2) with 27.5 and 22.3%, respectively, where crop residue burning is observed during post-monsoon (October–November) and winter (DJF) seasons (Kharol *et al*., 2012).

The interannual variation in the range of fog frequency across different stations of IGP is shown in Figure 2b. It is to be noted that while the 37-year average in Figure 2a shows frequency of 10–40%, higher frequency in later years is observed with maximum up to 60% as seen in Figure 2b. This reflects the local meteorological conditions as opposed to the fog anomaly time series (averaged over IGP and mean calculated with respect to the study period, 1977/1978–2013/2014) is shown in Figure S2. A surge in frequency (shift from negative to positive anomaly) is observed around the year 1997/1998. Figures 3 and 4 represent the interannual variation in associated meteorological variables. A decrease in temperature is also observed after 1996/1997 with the exception of years 2005–2009. The difference between maxima and minima of T_{dep} and diurnal temperature range (DTR) is higher during pre-1997 and narrows during post-1997 (Figure 3c and f). Also, along with an increase in fog frequency (Figure 2b), a corresponding decrease in Vis and increase in RH, particularly after year 1996/1997 can be seen in Figure 4a and b, respectively. A decrease in U after 1996/1997 is also observed in Figure 4c.

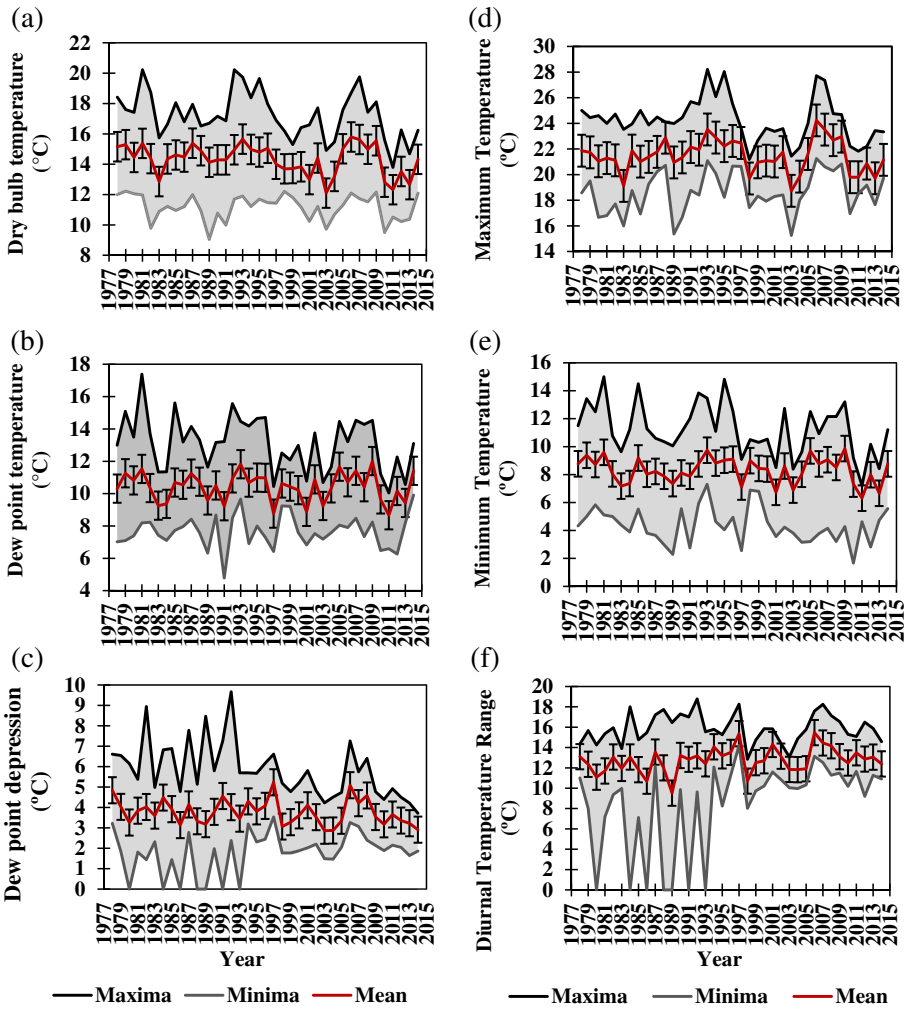

FIGURE 3 Time series for Tdb (a), Td (b), Tdep (c), Tamax (d), Tamin (e), and DTR (f) corresponding to the 10 stations. Mean (red), maxima (black) and minima (Grey); bars correspond to ±1 standard deviation. Each year corresponds to DJF, that is, January–February of that year and December of previous year [Colour figure can be viewed at wileyonlinelibrary.com]

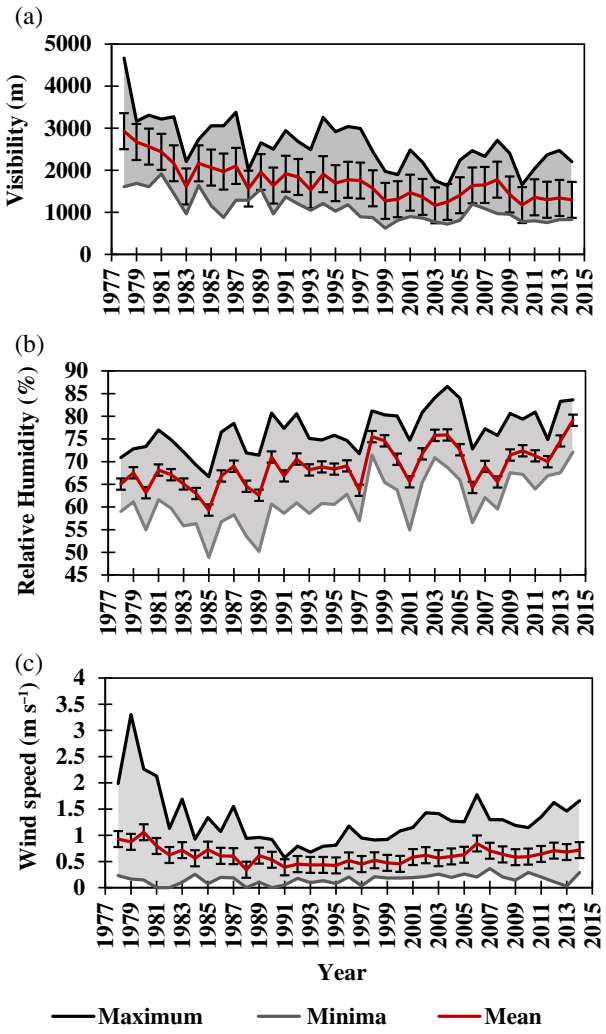

FIGURE 4 Time series for Vis (a), RH (b) and U (c) corresponding to the 10 stations. Mean (red), maxima (black) and minima (Grey); bars correspond to ±1 standard deviation. Each year corresponds to DJF, that is, January–February of that year and December of previous year [Colour figure can be viewed at wileyonlinelibrary.com]

3.1 | Presence of possible regimes during period of study

To explore the possible presence of regime shifts in the fog time series, RSI method proposed by Rodionov (2004) is used. Further, frequency analysis including EEMD and Fourier analysis are applied to determine the cut off length, L to be used in calculation of RSI. Figure S1a depicts the Vis time series during fog averaged over IGP for the study period. A decrease in Vis is observed post 1997. The IMFs obtained from EEMD are seen in b, with oscillations transitioning from fast to slow as we move from IMF1 to IMF4 and a decreasing trend of the series at the bottom. Figure S1c shows the Fourier analysis of the oscillatory components (IMFs 1–4) with peaks at 2.5, 9.7, 18.5, and 37 years, respectively. This quantifies the periodicity within

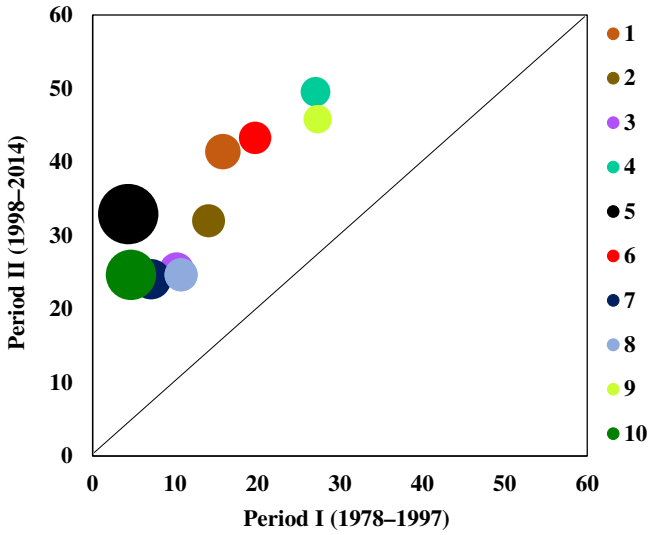

FIGURE 5 Scatter diagram depicting the frequency of fog days per DJF (%) corresponding to regime I (1978–1997) and II (1998–2014) over the 10 stations in IGP. The colour of bubbles corresponds to different stations and the size depicts the ratio of fog frequency for period II/I [Colour figure can be viewed at wileyonlinelibrary.com]

the time series. Statistical significance of IMFs calculated by plotting energy of IMFs (lnE) as a function of period (lnT) is seen in d. IMFs 2 and 4 corresponding to peaks 9.7 (~10) and 37 are significant. Therefore, the cut off length for RSI is taken as 10. The test for possible regimes within the study period following the RSI method reveals a regime shift at year 1997/1998. This is obtained as follows:

1. As detailed in the methodology, for $L = 10$ at probability level, $p = .05$ and 2L-2 degrees of freedom, critical value of Student's t distribution, $t = 2.1$ for two tailed test. The fog anomaly time series (Figure S2) is used for the analysis. For running 10 year intervals, average variance, $\sigma_L{}^2 = 50.01$ and difference, $D = 6.64$. The mean of first 10 years (1978–1987) is $\mu_{R1} = -12.54$.

2. To qualify as a regime shift, 11th year (1988, which corresponds to December of 1987 and January–February of 1988) must have a value exceeding $\mu'_{R2.}$ The new value should be greater than 6.64–12.54 = −5.9 or less than −12.54 − 6.64 = −19.18. As the value at year 1988 is −7.36, it cannot be considered as a regime shift.

3. The mean μ_{R1} is recalculated by including the next year, 1989 and L−1 (9) values of previous interval and corresponding μ'_{R2} is computed. The next value (corresponding to year 1990) must be greater than 6.64–11.77 = −5.13 or less than −11.77−6.64 = −18.41. As the value, −1.63 exceeds μ'_{R2}, 1990 is considered as the starting point of a new regime. The RSI value is computed as $RSI_{1990,1990}$ = (5.13–1.63)/7.07/10 = 0.04. However, $RSI_{1991,1990}$ = (5.13–13.86)/7.07/10 = −0.12. As the sign is opposite to that of the regime shift, the test at year $j = 1990$ has failed.

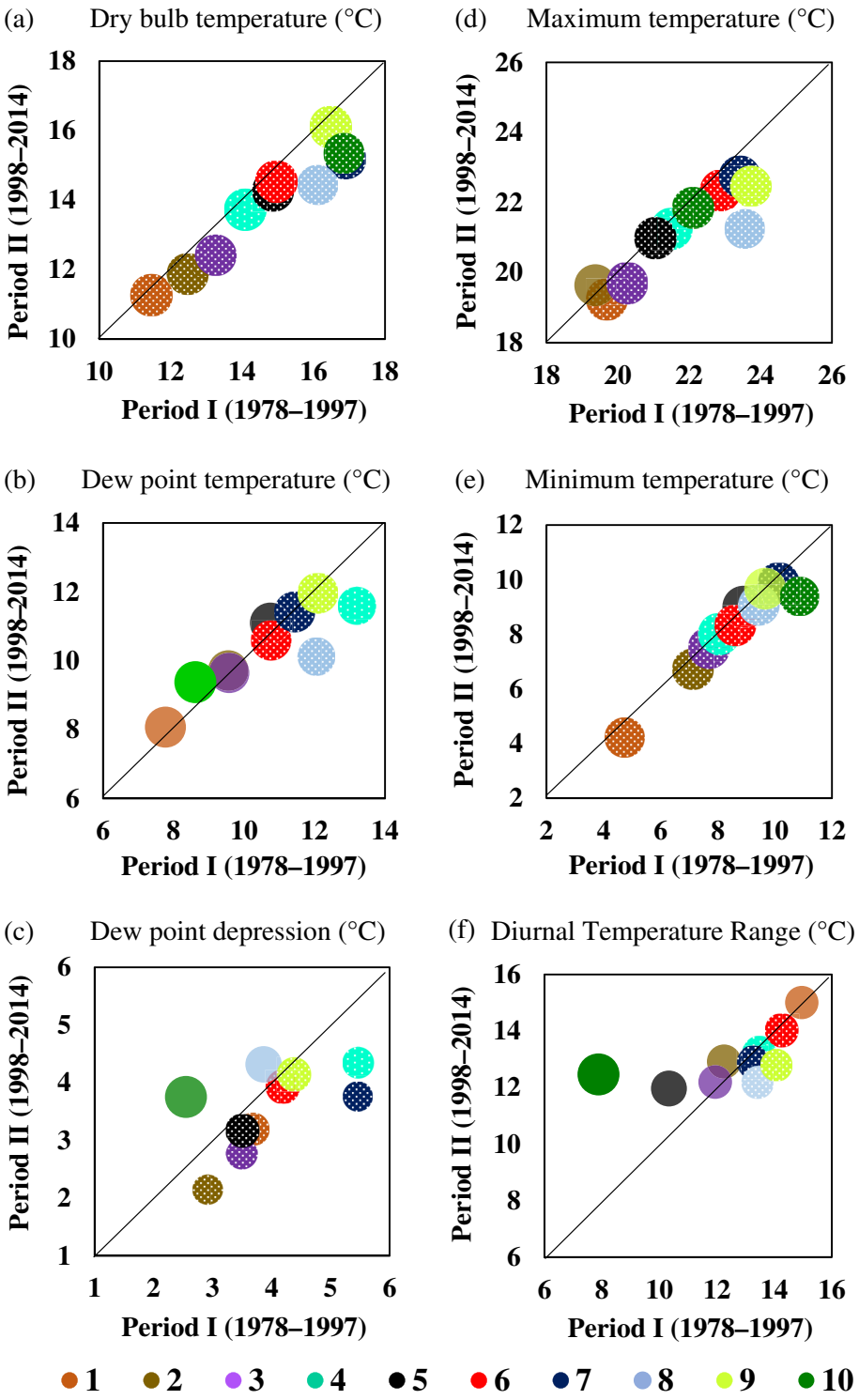

FIGURE 6 Scatter diagram depicting Tdb (a), Td (b), Tdep (c), Tamax (d), Tamin (e), and DTR (f) during fog days corresponding to I (1978–1997) and II (1998–2014) over the 10 stations in IGP. The colour of bubbles corresponds to different stations and the size depicts the ratio of fog frequency for period II/I. The bubbles with patterns correspond to a fractional decrease in values during II from I [Colour figure can be viewed at wileyonlinelibrary.com]

4. The mean μ_{R1} is recalculated and possible starting points of regime shifts are assessed using RSI. Out of 37 years of time series data, 14 years (1990, 1992, 1993, 1998, 1999, 2000, 2002, 2003, 2004, 2008, 2009, 2010, 2013, and 2014) are possible starting points but only 1998 has a sustainable shift of magnitude 0.12. This may be because the method detects abrupt shifts and may not detect more gradual transitions with lesser magnitudes. The shift is in agreement with the fog anomaly time series in Figure S2. Also, the spread between maxima and minima increases around 1997 (a strong El Nino year) in Figure 2b. Dimri (2013) found a significant correlation between northwest India winter precipitation (NWIWP) and the El Nino Southern Oscillation (ENSO) with increased precipitation during warm phase of ENSO. Yadav *et al.* (2009) have found that ENSO influence on the interannual variability of the

NWIWP by way of intensification of WDs has enhanced in the recent decades. WDs are major source of moisture in north west India including the IGP and are associated with both radiation and advection fog (Sawaisarje *et al.*, 2014). The present study also finds a concurrent increase in RH in regime II (1997/1998 to 2013/2014) as compared to regime I (1977/1978 to 1996/1997) (Figure 7b). The latter period has also witnessed a comparative increase in pollution which is reflected in the higher frequencies of fog at the major cities. All stations show similar interannual change in frequency.

3.2 | Trends in fog and associated meteorological variables

As distinct patterns are observed post 1996/1997, the two regimes are to be further analysed. Thus, the fog frequency and associated meteorological factors for the two regimes: 1977/1978–1996/1997 (Regime I) and 1997/1998–2013/2014 (Regime II) were compared for possible trends. Figure 5 shows a scatter plot between I and II. The fractional increase in fog frequency during II is of similar magnitude in most stations except Bareilly (5) and Gaya (10). Localized factors could be responsible for such exceptions. Also, changes in data measurement practices and missing values could also play a role. The increase in fog frequency during II is significant as per paired *t* test at 95% significance level along with an increasing trend (Sen slope 0.96). The Sen slope, by definition fits a line to sample points in a plane by choosing median of slopes of lines through pairs of points having distinct × coordinates. The method is less sensitive to outliers and therefore more robust than the least squares estimator for skewed and heteroskedastic data and fares well even for normally distributed data.

Trends developed in associated meteorological parameters for the two regimes is assessed and shown in Figures 6 and 7. A decrease in T_{db}, T_{amin}, and T_{amax} during II (significant at 95% level) is observed (Figure 6). The net radiative cooling exerted by fog at the top of atmosphere (Sathiyamoorthy *et al.*, 2016) could be a major reason for the observed decreasing trend in temperature during fog days together with increasing trend in fog frequency in regime II. Singh and Sontakke (2002) also found a significant decreasing trend in temperature over IGP in the post-1958 period and attributed it to expansion of agricultural activities and the spreading of irrigation network, in conjunction with increase and spatial shift in rainfall within IGP. Also, 8 out of 10 stations (Figure 6c) show a decreasing (not significant) trend in T_{dep} in II which is in agreement with this increase in rainfall and with increasing (not significant) trends in humidity (Figure 7b). The increase in fog frequency would lead to a significant decrease in Vis as seen in Figure 7a. Higher wind speeds disperse fog by mixing and eddies; therefore, calm conditions are considered suitable for radiation fog formation. Higher wind speeds are, however conducive for formation of advection fog. This condition is usually seen over the regions near warm ocean, but has been observed to occur over IGP prior to the passage of WDs, synoptic weather systems originating in the Mediterranean region and transporting moisture to Indian subcontinent during winter (Sawaisarje *et al.*, 2014). The wind speeds in majority of stations show an increasing trend (not significant) during II. Although wind speeds are

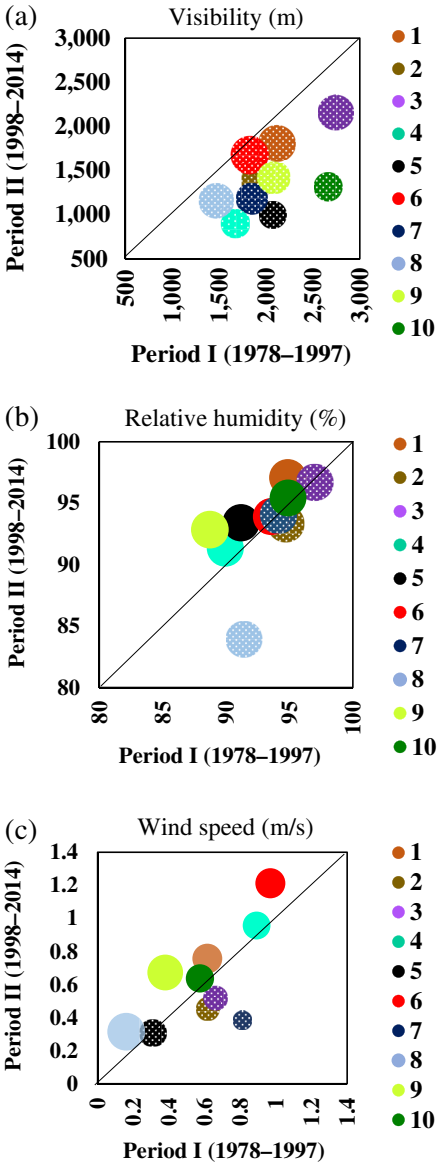

FIGURE 7 Scatter diagram depicting Vis (a), RH (b), and U (c) during fog days corresponding to I (1978–1997) and II (1998–2014) over the 10 stations in IGP. The colour of bubbles corresponds to different stations and the size depicts the ratio of fog frequency for II/I. The bubbles with patterns correspond to a fractional decrease in values during II from I. Significant decrease in Vis and increase in RH is observed during II [Colour figure can be viewed at wileyonlinelibrary.com]

higher during II, presence of other conditions that are conducive for fog formation including lower T_{db}, T_{amax} and T_{amin}, lower T_{dep}, and higher RH may contribute to enhance fog in regime II.

3.3 | Vis dependence on meteorological variables during fog versus non-fog conditions

Fog has an adverse impact on transportation sector including road, rail and aviation mainly due to low Vis. Understanding the extent to which meteorological factors influence Vis is important for fog forecasting studies. In an attempt to quantify Vis and its dependence on meteorological parameters during fog days, scatterplots of Vis with meteorological variables for fog and non-fog days at Amritsar (1) are shown in Figures 8, 9, and 10. Similar plots were drawn for all other stations as well but as similar patterns were observed, only one station is shown here for reference. As the values are daily averages, Vis during fog days is >1,000 m but suffices when considering the long-term climatological aspect and a comparison with non-fog days.

From Figures 8 and 9, it can be inferred that for the same temperature range of 4–10°C, there are more incidences of lower Vis in regime II (green) as opposed to regime I (red)

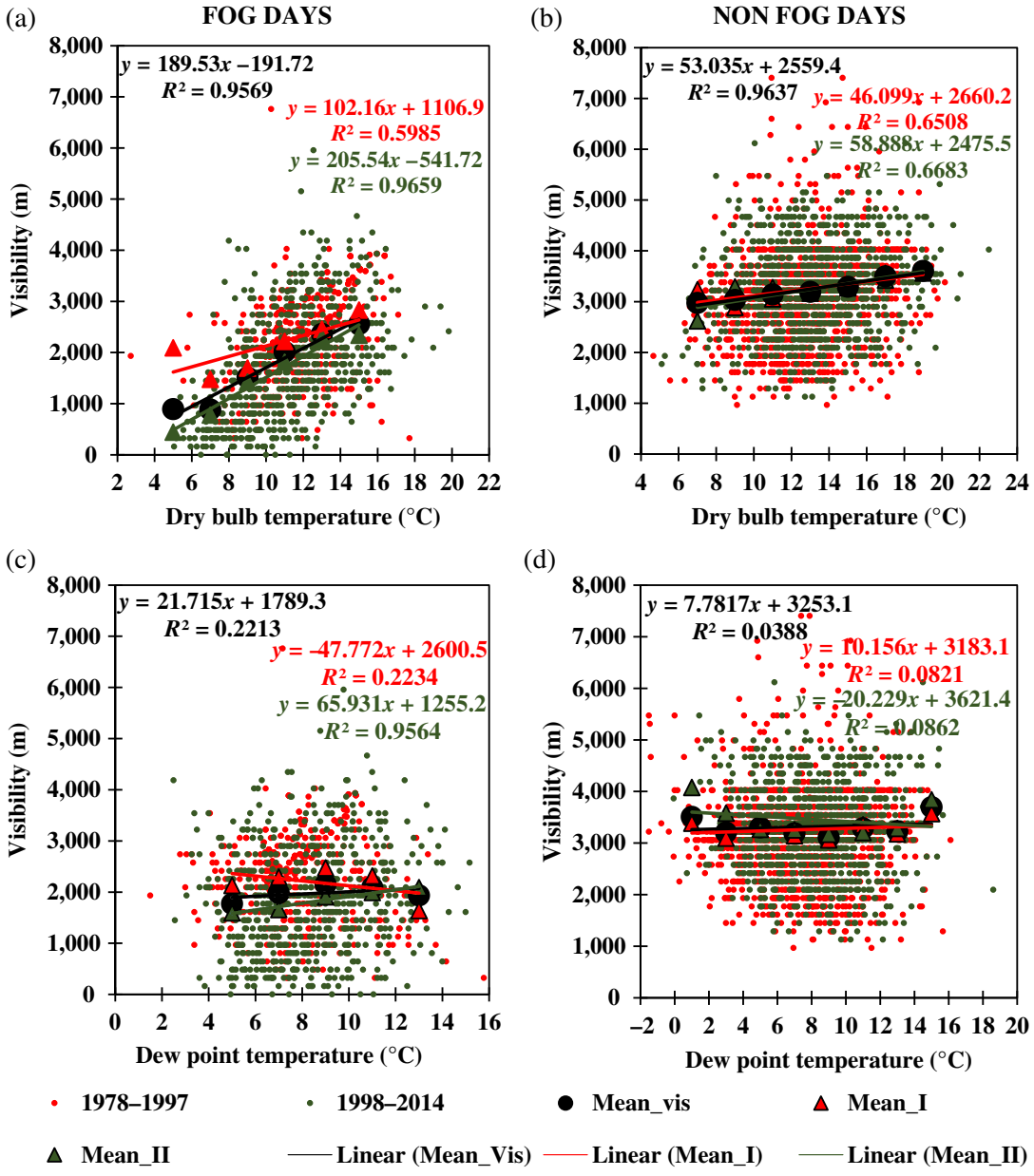

FIGURE 8 Scatterplot of Vis with Tdb (a) and (b), with Td (c) and (d) during fog (left) and non-fog days (right), respectively, for periods 1977/1978–1996/1997 and 1997/1998–2013/2014 over Amritsar. The circles correspond to mean Vis at dx = 2°C while triangles correspond to mean Vis during regimes I and II, respectively [Colour figure can be viewed at wileyonlinelibrary.com]

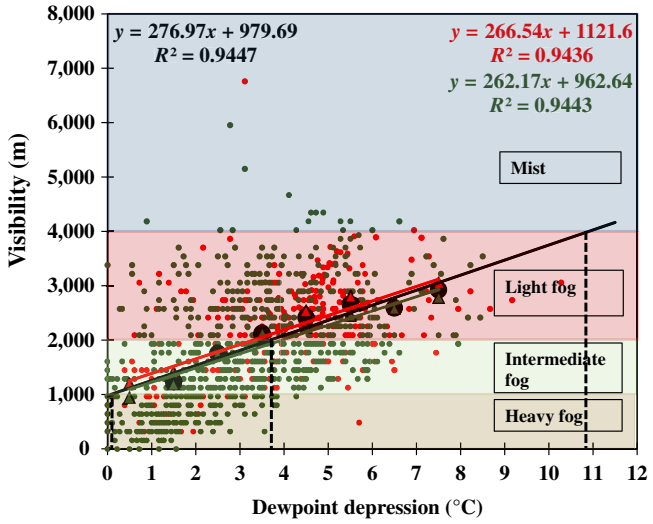

FIGURE 9 Scatterplot of Vis with Tdep during fog days for periods 1977/1978–1996/1997 (red) and 1997/1998–2013/2014 (green) over Amritsar. The circles correspond to mean Vis at dx = 1°C while triangles correspond to mean Vis during regimes I and II, respectively. Shaded regions represent weather types corresponding to Vis categories. Dashed lines correspond to Tdep = Tdb−Td at mean Vis 1000, 2000, and 4000 m [Colour figure can be viewed at wileyonlinelibrary.com]

during fog days (left panel) while the same cannot be said for non-fog days (right panel). Slopes corresponding to fog days are steeper in comparison to non-fog days indicating the strong influence of temperature over Vis due to fog. Also steeper slopes are observed for II as compared to I. The circles correspond to mean Vis at dx = 2°C while triangles correspond to regimes I (red) and II (green). While steeper slopes are observed in case of wind speed (R^2 = 0.64, Figure 10a), T_{db} (R^2 = 0.95, Figure 8a) and T_{amax} (R^2 = 0.91, Figure 10c); slopes are less steep in case of T_d (R^2 = 0.22, Figure 8c) and T_{amin} (R^2 = 0.49, Figure 10e). The magnitude and significance of the slopes can be inferred from Tables 1 and 2. In agreement with Figure 8, for the same wind speed range and temperature ranges, more incidences of lower Vis are seen in II (green) as opposed to I (red) during fog days (left) while the same cannot be said for non-fog days (right). Decrease in slope during II as compared to I in T_{amax} and T_{amin} and an increase in case of wind speed could indicate a weakened (strengthened) response of Vis to changes in temperature and wind speed due to increase in built up area or higher concentration of pollutants.

3.4 | Vis dependence on T_{dep}

In Figure 9, dx = 1°C and T_{dep} at mean Vis of 1,000, 2000, and 4,000 m are 0.075, 3.65, and 10.92°C, respectively, and indicated by dashed lines. Vis ≤1,000 m correspond to heavy fog conditions, Vis >1,000 m and <2000 m correspond to intermediate fog, Vis ≥2000 m and <4,000 m correspond to light fog and Vis ≥4,000 m indicates mist conditions. Higher incidences of heavy fog and mist are observed in regime II (Green). The fits, however do not show much change from regimes I to II indicating that the relation between Vis and T_{dep} has not changed considerably (see Tables 1 and 2). These tables quantify the slopes for fog and non-fog days in the two regimes. The significance of slope is based on regression analysis with Vis being the dependent variable and various meteorological parameters as independent variables. For a confidence level of 95%, *p*-value of *t*-statistic less than alpha value of 0.05 leads to rejection of null hypothesis (indicating the gradient is significant) and vice versa. The relation between Vis and T_{dep} is opposite to fits obtained for other variables. The slope for T_d is significant during regime II as opposed to regime I. Positive slope indicates that Vis will change in the direction of T_{dep}. Similarly, significant positive slopes for dVis/T_{db} indicates an increase in Vis with an increase in T_{db}. Higher value of slope of dVis/dT_{dep} during fog indicates greater rate of change as compared to non-fog days. This means that a decrease in T_{dep} would favour drop in Vis more during fog days as compared to non-fog days. The conducible conditions for fog dissipation by way of higher wind speeds existed during regime II but it may be compensated by the higher number of cloud condensation nuclei leading to fog formation when RH is near 100%. Thus, only a difference of ~4 is observed in the slopes. However, the intercept corresponding to Vis at T_{dep} = 0 is higher for regime I (>1,000 m) and lower for regime II (<1,000 m). This may indicate that at the same value of T_{dep}, Vis decreased from regime I to II in agreement with Figure 9a.

Lower slope for dVis/dT_{amax} during fog in II indicates the rate of decrease in Vis with respect to corresponding decrease in T_{amax} will be slower as opposed to *I*. The opposite is observed in case of T_{amin}.

The temporal variation in the extent of Vis dependence on meteorological parameters is inherent from the results. Significant changes in slopes (Tables 1 and 2) of Vis versus meteorological parameters (especially T_{db}, T_{dep}, and wind speed) during different regimes as well as fog and non-fog days are observed. An in-depth understanding of this dependence will provide a background for using these variables as proxy for Vis in climate and atmospheric applications. This is especially useful while analysing gridded data sets and selective station data analysis wherein there is a lack of Vis observations. Thus, when considering a model for fog over IGP based on Vis, it is imperative to keep in mind the differences in slopes and the extent of dependency of Vis on these parameters.

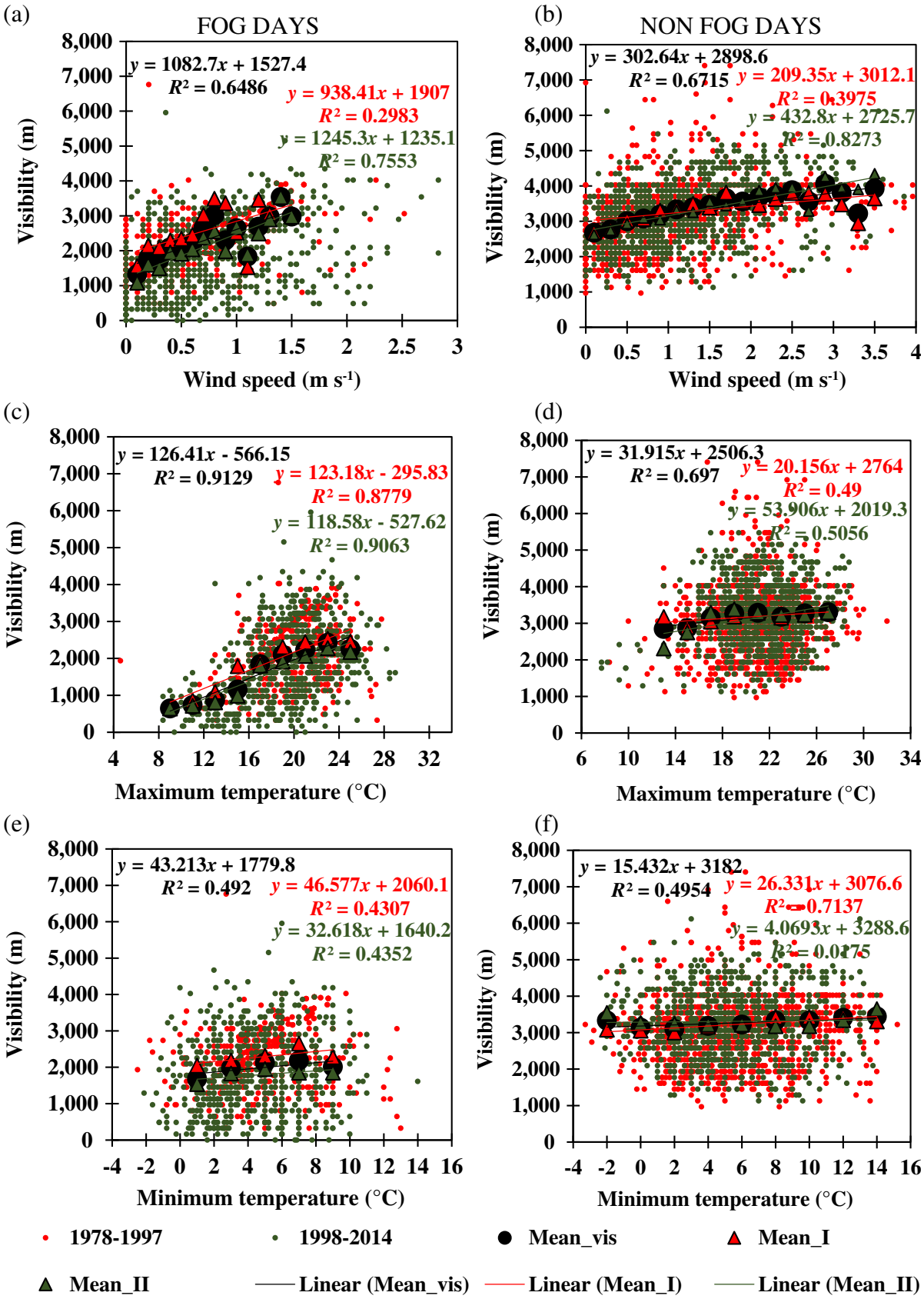

FIGURE 10 Scatterplot of Vis with U (a) and (b), with Tamax (c) and (d), with Tamin (e) and (f). The black circles correspond to mean Vis at dx = 2°C and 0.2 m·s^{-1} while triangles correspond to mean Vis during regimes I and II, respectively [Colour figure can be viewed at wileyonlinelibrary.com]

TABLE 1 Slopes of the fits shown in Figures 8 and 9 together with its significance. The level of significance is calculated based on *t* test at 95% confident interval

Slope	Event	Gradient [m·°C^{-1}]	Comments
dVis/dT$_{db}$	FG_mean	1,496.4/12	Significant
	FG_I	543.6/12	Significant
	FG_II	1810.5/12	Significant
	NFG_mean	1836.1/14	Significant
	NFG_I	1875.5/14	Significant
	NFG_II	1,782.3/14	Significant
dVis/dT$_{d}$	FG_mean	162.6/8	No
	FG_I	−489.3/8	No
	FG_II	492.0/8	Significant
	NFG_mean	188.7/14	No
	NFG_I	185.3/14	No
	NFG_II	−237.5/14	No
dVis/dT$_{dep}$	FG_mean	1925.0/7	Significant
	FG_I	1848.1/7	Significant
	FG_II	1836.6/7	Significant
	NFG_mean	922.0/10	Significant
	NFG_I	886.4/10	Significant
	NFG_II	1,042.5/10	Significant

TABLE 2 Slopes of fits shown in Figure 10 together with their significance. The level of significance is calculated based on *t* test at 95% confident interval

Slope	Event	Gradient [m/(m·s^{-1})]	Comments
dVis/dU	FG_mean	1,652.6/1.2	Significant
	FG_I	1,497.3/1.2	No
	FG_II	1814.2/1.2	Significant
	NFG_mean	992.2/3.8	Significant
	NFG_I	971.2/3.8	Significant
	NFG_II	1,075.7/3.8	Significant
Slope	Event	Gradient [m·°C^{-1}]	Comments
dVis/dT$_{amax}$	FG_mean	1,610.9/16	Significant
	FG_I	2,453.2/16	Significant
	FG_II	1,527.1/16	Significant
	NFG_mean	458.8/14	Significant
	NFG_I	131.9/14	No
	NFG_II	989.4/14	No
dVis/dT$_{amin}$	FG_mean	329.3/8	No
	FG_I	233.0/8	No
	FG_II	315.4/8	No
	NFG_mean	109.6/16	Significant
	NFG_I	224.8/16	Significant
	NFG_II	105.6/16	No

4 | CONCLUSIONS

The present study analysed long-term trends (over 37 years) in fog occurrence and associated meteorological factors. Then, results are assessed using presence of climatic regime shifts occurred in the year of 1997–1998. Based on extensive data analysis, following conclusions are drawn from the present study:

1. Fog frequency has increased over the IGP during the study period and a regime shift was observed in the year 1997/1998.
2. Fog Vis is classified based on T_{dep} (~RH) that is applicable for climate studies rather than aviation operations.
3. Significant changes in associated meteorological factors such as temperature, Vis, wind speed are seen during fog days in both the regimes. These include significant decrease in T_{db}, T_{amin}, and T_{amax} as well as in Vis in regime II as compared to regime I. When considering Vis versus meteorological factors, steeper slopes are observed during fog days in regime II as opposed to I in case of T_{db}, T_d, T_{amin}, and wind speed.
4. Based on air temperature changes possible over more than 50 years based on climate simulations (Basha *et al*., 2017), the present work Vis values can improve up to 1 km (Figure 8) but fog occurrence increased significantly (Figure 2).
5. The most important parameters affecting the fog occurrence are found to be air temperature, wind speed, and mixing ratio. Therefore, increasing fog occurrence were likely due to saturation (RH~100%) of boundary layer because of likely increasing day of cooler temperatures during winter (not long-term averages), as well as abundance of nucleating aerosols.
6. Vis decreased more than 1,000 m since 1970s during winter months and found to be associated with increasing RH and low wind speed conditions (e.g., <1.5 m s^{-1}).
7. The two regimes have distinct fog patterns and indicate changes in strength of association with changing meteorological parameters and likely due to anthropogenic aerosol effects for example, cloud condensation nuclei due to farming in the region. Therefore, attempts at fog prediction should take into consideration these changes as models that may work well in one regime but may not perform satisfactorily in a different regime.

Fog occurrence depends on various meteorological, topographical, aerosol, radiation, saturation level of lower atmospheric boundary layer, and forcing conditions for cooling processes (Gultepe *et al*., 2007). Because of its lower magnitude of physical components, fog prediction needs diligent and accurate measurements and data processing for prediction

applications. Therefore, for evaluation of the fog occurrence conditions, detailed field studies on fog microphysical processes and forcing mechanism are needed. Then, climate model simulations can be performed to explain what is happening fog physical processes over the IGP region, and advised if the results are applicable to other parts of the world.

ACKNOWLEDGEMENTS

The first author acknowledges the University Grants Commission funding for Senior Research Fellowship and Jawaharlal Nehru University for providing the requisite facilities as part of the UPoE-II scheme. The authors acknowledge National Centers for Environment Information, National Oceanic and Atmospheric Administration for providing access to the data set.

ORCID

Ashok Priyadarshan Dimri https://orcid.org/0000-0002-7832-8669

REFERENCES

Arun, S.H., Chaurasia, S., Misra, A. and Kumar, R. (2018) Fog stability index: a novel technique for fog/low clouds detection using multi-satellites data over the Indo-Gangetic plains during winter season. *International Journal of Remote Sensing*, 39(22), 8200–8218.

Basha, G., Kishore, P., Ratnam, M.V., Jayaraman, A., Kouchak, A.A., Ouarda, T.B. and Velicogna, I. (2017) Historical and projected surface temperature over India during the 20 th and 21 st century. *Scientific Reports*, 7(1), 2987.

Bhowmik, S.K.R., Sud, A.M. and Singh, C. (2004) Forecasting fog over Delhi-an objective method. *Mausam*, 55(2), 313–322.

Business Standard. 2013. *Foggy weather affects vegetable, fruit crops*. Published January 20, 2013. Available at: https://www.business-standard.com/article/economy-policy/foggy-weather-affects-vegetable-fruit-crops-110012500064_1.html [Accessed 26th August 2018].

Chaudhuri, S., Das, D., Sarkar, I. and Goswami, S. (2015) Multilayer perceptron model for nowcasting visibility from surface observations: results and sensitivity to dissimilar station altitudes. *Pure and Applied Geophysics*, 172(10), 2813–2829.

Di Girolamo, L., Bond, T.C., Bramer, D., Diner, D.J., Fettinger, F., Kahn, R.A., Martonchik, J.V., Ramana, M.V., Ramanathan, V. and Rasch, P.J. (2004) Analysis of Multi-angle Imaging Spectro Radiometer (MISR) aerosol optical depths over greater India during winter 2001–2004. *Geophysical Research Letters*, 31(23). https://doi.org/10.1029/2004GL021273.

Dimri, A.P. (2013) Relationship between ENSO phases with Northwest India winter precipitation. *International Journal of Climatology*, 33 (8), 1917–1923.

Dupont, J.C., Haeffelin, M., Stolaki, S. and Elias, T. (2016) Analysis of dynamical and thermal processes driving fog and quasi-fog life cycles using the 2010–2013 ParisFog dataset. *Pure and Applied Geophysics*, 173(4), 1337–1358.

Dutta, D. and Chaudhuri, S. (2015) Nowcasting visibility during wintertime fog over the airport of a metropolis of India: decision tree algorithm and artificial neural network approach. *Natural Hazards*, 75(2), 1349–1368.

Ganguly, D., Rasch, P.J., Wang, H. and Yoon, J.H. (2012) Climate response of the South Asian monsoon system to anthropogenic aerosols. *Journal of Geophysical Research: Atmospheres*, 117 (D13) https://doi.org/10.1029/2012JD017508.

Gautam, R. and Singh, M.K. (2018) Urban heat Island over Delhi punches holes in widespread fog in the Indo-Gangetic Plains. *Geophysical Research Letters*, 45(2), 1114–1121.

Gautam, R., Hsu, N.C., Kafatos, M. and Tsay, S.C. (2007) Influences of winter haze on fog/low cloud over the Indo-Gangetic plains. *Journal of Geophysical Research: Atmospheres*, 112(D5). https://doi.org/10.1029/2005JD007036.

Ghude, S.D., Bhat, G.S., Prabhakaran, T., Jenamani, R.K., Chate, D.M., Safai, P.D., Karipot, A.K., Konwar, M., Pithani, P., Sinha, V. and Rao, P.S.P. (2017) Winter fog experiment over the Indo-Gangetic plains of India. *Current Science* (00113891), 112(4), 767–784.

Giulianelli, L., Gilardoni, S., Tarozzi, L., Rinaldi, M., Decesari, S., Carbone, C., Facchini, M.C. and Fuzzi, S. (2014) Fog occurrence and chemical composition in the Po valley over the last twenty years. *Atmospheric Environment*, 98, 394–401.

Gultepe, I., Muller, M.D. and Boybey, Z. (2006) A new warm fog parameterization scheme for numerical weather prediction models. *Journal of Applied Meteorology*, 45, 1469–1480.

Gultepe, I., Tardif, R., Michaelides, S.C., Cermak, J., Bott, A., Bendix, J., Müller, M., Pagowski, M., Hansen, B., Ellrod, G., Jacobs, W., Toth, G. and Cober, S.G. (2007) Fog research: a review of past achievements and future perspectives. *Journal of Pure and Applied Geophysics*, Special issue on fog, edited by I. Gultepe, 164, 1121–1159.

Gultepe, I., Minnis, P., Milbrandt, J., Cober, S.G., Nguyen, L., Flynn, C. and Hansen, B. (2008) The fog remote sensing and modeling (FRAM) field project: visibility analysis and remote sensing of fog. In: *Remote Sensing Applications for Aviation Weather Hazard Detection and Decision Support*. Optical Engineering + Applications: San Diego, California, Vol. 7088. International Society for Optics and Photonics, p. 708803.

Gultepe, I., Pearson, G., Milbrandt, J.A., Hansen, B., Platnick, S., Taylor, P., Gordon, M., Oakley, J.P. and Cober, S.G. (2009) The fog remote sensing and modeling field project. *Bulletin of the American Meteorological Society*, 90(3), 341–360.

Gultepe, I., Sharman,R., Williams, P. D., Zhou, B., Ellrod, G., Minnis, P., Trier, S., Griffin, S.,Yum, S. S., Gharabaghi, B., Feltz, W., Temimi, M., Pu, Z., Storer L. N., Kneringer, P., Weston, M. J., Chuang, H., Thobois, L., Dimri, A. P., Dietz, S. J., Franca, G. B., Almeida, M. V. and Albquerque Neto, F. L. (2018) A review of high impact weather for aviation meteorology. *Pure and Applied Geophysics* Accepted, 176(5), 1869–1921.

Jenamani, R.K. (2007) Alarming rise in fog and pollution causing a fall in maximum temperature over Delhi. *Current Science* (00113891), 93(3), 314–322.

Kaskaoutis, D.G., Houssos, E.E., Goto, D., Bartzokas, A., Nastos, P.T., Sinha, P.R., Kharol, S.K., Kosmopoulos, P.G., Singh, R.P. and Takemura, T. (2014) Synoptic weather conditions and aerosol episodes over Indo-Gangetic Plains, India. *Climate Dynamics*, 43 (9–10), 2313–2331.

Kendall, M.G. (1938) A new measure of rank correlation. *Biometrika*, 30(1/2), 81–93.

Kharol, S.K., Badarinath, K.V.S., Sharma, A.R., Mahalakshmi, D.V., Singh, D. and Prasad, V.K. (2012) Black carbon aerosol variations over Patiala city, Punjab, India—a study during agriculture crop residue burning period using ground measurements and satellite data. *Journal of Atmospheric and Solar-Terrestrial Physics*, 84, 45–51.

LaDochy, S. (2005) The disappearance of dense fog in Los Angeles: another urban impact? *Physical Geography*, 26(3), 177–191.

Madan, O.P., Ravi, N. and Mohanty, U.C. (2000) A method for forecasting of visibility at Hindon. *Mausam*, 51(1), 47–56.

Mohapatra, M. and Thulasi Das, A. (1998) Analysis and forecasting of fog over Bangalore airport. *Mausam*, 49, 135–142.

Price, J.D., Lane, S., Boutle, I.A., Smith, D.K.E., Bergot, T., Lac, C., Duconge, L., McGregor, J., Kerr-Munslow, A., Pickering, M. and Clark, R. (2018) LANFEX: a field and modeling study to improve our understanding and forecasting of radiation fog. *Bulletin of the American Meteorological Society*, 99(10), 2061–2077.

Rodionov, S.N. (2004) A sequential algorithm for testing climate regime shifts. *Geophysical Research Letters*, 31(9) https://doi.org/10.1029/2004GL019448.

Sathiyamoorthy, V., Arya, R. and Kishtawal, C.M. (2016) Radiative characteristics of fog over the Indo-Gangetic Plains during northern winter. *Climate Dynamics*, 47(5–6), 1793–1806.

Sawaisarje, G.K., Khare, P., Shirke, C.Y., Deepakumar, S. and Narkhede, N.M. (2014) Study of winter fog over Indian subcontinent: climatological perspectives. *Mausam*, 65(1), 19–28.

Sen, P.K. (1968) Estimates of the regression coefficient based on Kendall's tau. *Journal of the American Statistical Association*, 63 (324), 1379–1389.

Singh, N. and Sontakke, N.A. (2002) On climatic fluctuations and environmental changes of the Indo-Gangetic plains India. *Climatic Change*, 52(3), 287–313.

Singh, A., George, J.P. and Iyengar, G.R. (2018) Prediction of fog/-visibility over India using NWP model. *Journal of Earth System Science*, 127(2), 26.

Srivastava, S.K., Sharma, A.R. and Sachdeva, K. (2016) Spatial and temporal variability of fog over the Indo-Gangetic Plains, India. *World Academy of Science, Engineering and Technology, International Journal of Environmental, Chemical, Ecological, Geological and Geophysical Engineering*, 10(11), 1042–1057.

Syed, F.S., Körnich, H. and Tjernström, M. (2012) On the fog variability over South Asia. *Climate Dynamics*, 39(12), 2993–3005.

The Economic Times. 2017 *Over 3000 trains delayed due to fog in Nov-Dec: Indian Railways*. Published December 27, 2017. Available at: https://economictimes.indiatimes.com/industry/transportation/railways/over-3000-trains-delayed-due-to-fog-in-nov-dec-indian-railways/articleshow/62272221.cms [Accessed 26th August 2018].

Witiw, M.R. and LaDochy, S. (2008) Trends in fog frequencies in the Los Angeles Basin. *Atmospheric Research*, 87(3–4), 293–300.

Wu, Z. and Huang, N.E. (2009) Ensemble empirical mode decomposition: a noise-assisted data analysis method. *Advances in Adaptive Data Analysis*, 1(01), 1–41.

Yadav, R.K., Rupa Kumar, K. and Rajeevan, M. (2009) Increasing influence of ENSO and decreasing influence of AO/NAO in the recent decades over Northwest India winter precipitation. *Journal of Geophysical Research: Atmospheres*, 114(D12). https://doi.org/10.1029/2008JD011318.

Zhou, B. and Du, J. (2010) Fog prediction from a multimodel mesoscale ensemble prediction system. *Weather and Forecasting*, 25(1), 303–322.

SUPPORTING INFORMATION

Additional supporting information may be found online in the Supporting Information section at the end of this article.

How to cite this article: Kutty SG, Dimri AP, Gultepe I. Climatic trends in fog occurrence over the Indo-Gangetic plains. *Int J Climatol*. 2020;40: 2048–2061. https://doi.org/10.1002/joc.6317